

21140

NATIONAL LIBRARY
OTTAWA



BIBLIOTHÈQUE NATIONALE
OTTAWA

NAME OF AUTHOR..... BING-JING WU

TITLE OF THESIS..... Hydrates... in... the... Methane... Isobutane...
System... and... in... liquefied... light...
Hydrocarbon... Mixtures.....

UNIVERSITY..... The... University... of... Alberta.....

DEGREE FOR WHICH THESIS WAS PRESENTED..... M.S.C.....

YEAR THIS DEGREE GRANTED..... 1974.....

Permission is hereby granted to THE NATIONAL LIBRARY
OF CANADA to microfilm this thesis and to lend or sell copies
of the film.

The author reserves other publication rights, and
neither the thesis nor extensive extracts from it may be
printed or otherwise reproduced without the author's
written permission.

(Signed).....

Bing-Jing Wu

PERMANENT ADDRESS:

Dept. of Chem. Eng.....
U. of A... Edmonton.....
Alta.....

DATED. May 7..... 1974

NL-91 (10-68)

THE UNIVERSITY OF ALBERTA
HYDRATES IN THE METHANE-ISOBUTANE SYSTEM AND
IN LIQUEFIED LIGHT HYDROCARBON MIXTURES

by



BING-JING WU

A THESIS

SUBMITTED TO THE FACULTY OF GRADUATE STUDIES AND RESEARCH
IN PARTIAL FULFILMENT OF THE REQUIREMENTS FOR THE DEGREE
OF MASTER OF SCIENCE IN CHEMICAL ENGINEERING

Department of Chemical Engineering

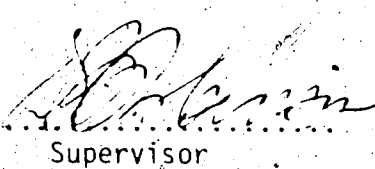
EDMONTON, ALBERTA

SPRING, 1974

THE UNIVERSITY OF ALBERTA

FACULTY OF GRADUATE STUDIES AND RESEARCH

The undersigned certify that they have read, and recommend to the Faculty of Graduate Studies and Research for acceptance, a thesis entitled "HYDRATES IN THE METHANE-ISOBUTANE SYSTEM AND IN LIQUEFIED LIGHT HYDROCARBON MIXTURES" submitted by BING-JING WU in partial fulfillment of the requirements for the degree of Master of Science in Chemical Engineering.


Supervisor

Date May 2, 1974

TO SOPHIA

ABSTRACT

Experimental data for gas hydrate formation in the methane-isobutane-water system have been obtained over a range of gas phase compositions from 0.4 to 63.6 mole percent isobutane. The highest composition for which data previously existed was 4.6 percent isobutane. The range of experimental pressures was from 23.0 to 1,460 psia and the range of temperature was from 33.2 to 68.8°F. Experimental data were also obtained on the initial hydrate formation conditions for the water rich liquid-hydrocarbon rich liquid-hydrate equilibrium for three mixtures of light hydrocarbons containing methane, ethane, propane and isobutane.

A recently proposed prediction method based on the Kihara cell potential model has been used to predict gas hydrate formation conditions with mixtures of methane and isobutane. The predicted pressures agreed well with experimental values at high isobutane concentrations but were considerably higher than the experimental values at lower compositions. For the liquefied hydrocarbon mixtures, the predicted temperatures were within 2.8°F of the experimental values at the bubble point pressures.

ACKNOWLEDGEMENT

The author wishes to express his thanks to Dr. D. B. Robinson for his guidance, advice and encouragement throughout the course of this investigation.

The author also appreciates the assistance received from the staff of the Chemical Engineering machine and instrument shops who constructed the equipment, from Mr. J. P. Moser who assisted with the analysis, from Mr. Hans Rempis who assisted with the equipment start-up, and from Mrs. M. R. Ruggles who typed the manuscript.

Financial assistance from the Petroleum Recovery Research Aid to Education Plan is gratefully acknowledged.

TABLE OF CONTENTS

	<u>Page</u>
<u>LIST OF FIGURES</u>	ix
<u>LIST OF TABLES</u>	x
<u>1. INTRODUCTION</u>	1
<u>2. LITERATURE REVIEW</u>	3
<u>3. THEORY</u>	7
A. Phase Behavior for Gas Hydrates	7
B. Use of Statistical Mechanical Theory in Gas Hydrate Studies	10
C. Numerical Method for the Prediction of Hydrate Formation Conditions	12
<u>4. EXPERIMENTAL METHODS</u>	15
A. Experimental Apparatus and Materials	15
(1) Equipment	15
(2) Control and Measurement of Temperature	18
(3) Measurement of Pressure	18
(4) Materials	19
B. Experimental Techniques	19
(1) Preparation of Mixtures	19
(2) Hydrate Formation	20
(3) Gas Chromatographic Analysis	21
<u>5. EXPERIMENTAL RESULTS</u>	23
A. Methane-Isobutane-Water System	23
B. Hydrates of Liquefied Light Hydrocarbon Mixtures	23

	Page
6. THEORETICAL RESULTS	27
A. Hydrate Formation Prediction for Methane-Isobutane-Water System	27
B. Hydrate Formation Prediction for Liquefied Hydrocarbon Gas Mixtures	27
7. DISCUSSION AND CONCLUSION	29
A. Validity of Experimental Data	29
B. Methane-Isobutane-Water System	29
C. Liquid Hydrocarbon Mixtures	30
D. Conclusion	30
8. FUTURE WORK	31
NOMENCLATURE	32
BIBLIOGRAPHY	35
APPENDICES	
A. Data Pertaining to Hydrate Physical and Molecular Structure	37
B. Experimental and Published Data	40
C. Computer Program for Gas Hydrate Formation Prediction	50

LIST OF FIGURES

No.		Page
1.	Qualitative Representation of Phase Behavior of the Ternary System CH_4 - $i\text{-C}_4\text{H}_{10}$ - H_2O for Hydrate Formation.	9
2.	Schematic Diagram for the Equipment.	16
3.	Schematic Diagram for the Trunnion.	17
4.	Gas Chromatograph Standardization	22
5.	Conditions for the Ternary CH_4 - $i\text{-C}_4\text{H}_{10}$ - H_2O System in $\text{H-L}_1\text{-G}$ Phase Equilibrium.	24
6.	Conditions for the Liquefied Light Hydrocarbon Mixtures in $\text{L}_1\text{-L}_2\text{-H}$ Equilibrium.	25

LIST OF TABLES

No.		Page
1.	Physical Properties of Hydrate Lattice	38
2.	Constants for Calculating Dissociation Pressures of Reference Hydrate	38
3.	Thermodynamic Properties of Empty Hydrate (β -phase) and Liquid Water Relative to Ice (α -phase) at 0°C and Zero Pressure	39
4.	Kihara Parameters for Hydrate-Gas Interactions	39
5.	Experimental Data for Methane-Isobutane Mixtures - Hydrate Formation in H-L ₁ -G Equilibrium	41
6.	Comparison of Methane Hydrate Formation Conditions (H-L ₁ -G) of the Published Data and This Work	43
7.	Published Experimental Data of Isobutane Hydrate Formation Condition in H-L ₁ -G Equilibrium	44
8.	Published Experimental Data of Methane-Isobutane Hydrate Formation Conditions in H-L ₁ -G Equilibrium	45
9.	Composition of Liquefied Hydrocarbon Mixtures	46
10.	Hydrate Formation Conditions for Three Liquefied Mixtures	46
11.	Predicted Hydrate Formation of Methane-Isobutane Mixtures in H-L ₁ -G Equilibrium	47
12.	Comparison between Experimental and Calculated Hydrate-Formation Conditions at Bubble Points for Liquid Mixtures	49

CHAPTER 1

INTRODUCTION

Gas hydrates, resembling snow or loose ice in appearance, are solid crystalline substances having the general formula M_nH_2O , where one or more hydrate-forming molecules M associate with n "host" water molecules. The metastable water crystal lattice is stabilized by physical forces between the "host" and "guest" molecules.

The important role of gas hydrates in gas processing industries was first realized in 1934 when Hammerschmidt [1] discovered that the hydrates of methane, ethane, propane and isobutane were responsible for the difficulties in the natural gas industry in the measurement and transportation of the gas. The movement of the gas through the pipeline tends to collect and compress the hydrate at low spots until the line may become entirely plugged. Research for the prevention of hydrate formation and, consequently, dehydration of the gas, has been carried out since that time. Considerable effort has been expended in finding the conditions of temperature and pressure at which hydrate will form, as well as in determining the equilibrium moisture content data for the gas. There is additional interest in gas hydrate formation connected with a series of processes which are carried out in other industries, for example, in distillation columns due to accumulated moisture and in heavy water production processes involving mixtures of hydrogen sulfide and water. Several prospective applications for the industrial use of gas hydrate include (1) the desalination of sea water; (2) the storage of gases; (3) the separation of gas and liquid mixtures. Therefore, the prediction of initial hydrate formation

condition becomes important in relation to several industrial processes.

There are many experimental data reported in the literature for gas hydrate formation conditions. By using these reported data several prediction methods have been developed and evaluated for their usefulness. Although much data exists, that available for mixtures of methane and isobutane is very scanty. Therefore, one objective of this work was to extend and complete the hydrate formation data for methane-isobutane mixtures.

Recent work, notably that of Parrish and Prausnitz [2], in developing a prediction method based on the statistical-mechanical theory of hydrate formation has opened the way to more effectively predicting hydrate formation in gas-liquid systems and has made it possible to attempt the prediction of hydrate formation in liquid-liquid systems. Consequently, another objective of this work was to investigate the phase behavior of hydrate formation conditions for liquefied light hydrocarbons and to determine at what condition and for what kinds of components in the mixtures hydrate formation conditions can properly be predicted with the new method.

CHAPTER 2

LITERATURE REVIEW

Von Stackelberg and Muller [3,4], Claussen [5,6], Pauling and Marsh [7], and Jeffrey and McMullan [8] studied the crystal structures of gas hydrates and concluded that for most nonpolar and some weakly polar molecules gas hydrates crystallise in either of two structures, referred to as Structure I and Structure II. The physical properties of these structures are given in Table 1. The structure formed depends primarily on the size of the guest molecule. When the effective diameter of the hydrate-forming molecules is less than 5.1 Å, all the cavities in hydrate Structure I can be filled and the ideal formula would be $M_1 \cdot 5\frac{3}{4} H_2O$ ($M_1 = Ar, Kr, CH_4, H_2S$, etc.). If the effective diameter of the hydrate-forming molecule is less than 5.8 Å but greater than 5.1 Å then the hydrate-forming molecules can fill only six large cavities and would have the ideal formula $M_2 \cdot 7\frac{2}{3} H_2O$ ($M_2 = SO_2, C_2H_4, C_2H_6, Cl_2, Br_2$, etc.). When two types of molecules are present simultaneously in the gas mixture, also called "mixed hydrate", with the ideal formula $2M_1 \cdot 6M_2 \cdot 46H_2O$ will form. Similarly, if the effective diameter of the hydrate-forming molecules is greater than 5.8 Å but less than 6.7 Å ($M_4 = C_3H_8, i-C_4H_{10}, CH_2Br_2$, etc.) a hydrate Structure II will form with the ideal formula $M_4 \cdot 17H_2O$. For a mixture $M_3 + M_4$, if the effective diameter of M_3 is less than 5.0 Å, the "mixed hydrate" will form with the ideal formula $2M_3 \cdot M_4 \cdot 17H_2O$. Both types of mixed hydrates are considered as solid solutions [9] in which the smaller molecules help to stabilize the hydrate structure. Any gas having a

molecular dimension larger than 6.7 Å such as n-butane and larger molecules are too big to form hydrates. It has been found that the quantum-gas molecules (helium, hydrogen, neon) are too small to form either hydrates I or II because they are not retained within the lattice very strongly. Byk and Fomina [10] have given a very extensive literature review on hydrates.

Wilcox, Carson and Katz [11,12] proposed an empirical method for predicting hydrate formation conditions through the use of solid-vapor equilibrium ratios. This method supposes that the solid-vapor equilibrium ratio is analogous to the liquid-vapor equilibrium ratio and based on the idea that the hydrates form solid solutions. Furthermore, the method assumes that the solid-vapor equilibrium ratio is independent of the overall composition of the mixture from which the hydrate has been formed. Even though it is now known that this premise is erroneous, the equilibrium ratio concept is useful in dealing with mixtures of reasonably uniform compositions such as those which may be found in natural gas production and transportation. Unreliable results will be obtained whenever the hydrate-forming mixtures are greatly different from those for which the solid-vapour equilibrium ratios were obtained. A set of charts presenting equilibrium ratios for methane, ethane, propane, isobutane, carbon dioxide, and hydrogen sulfide is available in the Gas Products Association Engineering Data Book [13]. The lack of experimental data on which the isobutane equilibrium ratios were based tends to make them subject to serious error.

Van der Waals and Platteeuw [9] used statistical mechanical principles to derive the thermodynamic properties of gas hydrates.

from a simple model by applying Lennard-Jones-Devonshire cell theory.

McKoy and Sinanoglu [14] calculated and compared dissociation pressures of some gas hydrates using the Lennard-Jones 12-6, 28-7 and Kihara potentials in the Lennard-Jones-Devonshire cell model. They found that the Kihara potential predicted better dissociation pressures for hydrates formed from rod-shaped molecules. The LJ 28-7 potential model gives only a qualitative indication of the effect of narrowing the potential bowl on dissociation pressures, that is, in going from LJ 12-6 to LJ 28-7, the dissociation pressures become higher. The LJ 12-6 potential does not depend on the shape and size of the interacting molecules. The model predicts good hydrate dissociation pressures for monatomic gases such as xenon and krypton but not for nonspherical and diatomic gases like CO_2 , N_2 , O_2 or C_2H_4 .

Kobayashi and co-workers [15,16] modified the equations of van der Waals and Platteeuw [9] and proposed a method of calculating several thermodynamic properties of gas hydrates above the lower quadruple point by using LJ 12-6 potential. They obtained excellent agreement between the calculated and experimental data for pure gas hydrates. Later, Nagata and Kobayashi [17,18] used the Kihara potential to make similar calculations for both pure gas hydrates and mixtures. For this work they obtained parameters for the Kihara model from the literature. Their results agree well with experimental data and are better than those obtained by using the LJ 12-6 potential.

Parrish and Prausnitz [2] used a similar approach but they applied numerical methods to fit a new set of values of the thermodynamic properties of the empty hydrate lattice and the Kihara parameters for 15 hydrate-forming gases. By using this method the agreement between

calculated and experimental data for many gas mixtures is better than it is for other previous methods.

The hydrate formation condition for the binary system of methane and water has been reported in the literature by Villard [19,20], Deaton and Frost [21,22], Roberts et al [23,24], Kobayashi and Katz [25,26], Campbell and McLeod [27], Otto and Robinson [28], and Marshall and co-workers [29]. Deaton and Frost [21] obtained the first reliable isobutane hydrate experimental data. Layano and Utida [30], and Rouher and Barduhn [31] have made a careful investigation of isobutane hydrate and determined its composition and quadruple points. Deaton and Frost [21] and Campbell and McLeod [27] investigated hydrate-forming conditions in the ternary system $\text{CH}_4\text{-i-C}_4\text{H}_{10}\text{-H}_2\text{O}$ for a few low concentrations of isobutane. In all cases, the isobutane concentration was less than 4/6 mole percent.

CHAPTER 3

THEORY

A. Phase Behavior of Hydrates

The Phase Rule is based on thermodynamic principles. It was first stated by Josiah Willard Gibbs [32] and it relates the number of phases (P), the number of components (C), and the number of degrees of freedom, or the variances (F) of a system in heterogeneous equilibrium by the mathematical relationship:

$$F = C - P + 2$$

The only measured variables used in this equation are temperature, pressure and composition. The relationship deals with the heterogeneous equilibrium encountered in processes which may be classified either as physical or chemical, as long as they are dynamic and reversible in nature. In contrast it does not apply to the typical static equilibrium states found in mechanics.

The Phase Rule deals with the phase behavior of a system as affected by changes in the variables for temperature, pressure, and composition. Composition refers to the proportions of the various components in the system and not really to the number and nature of these components. In a system where the composition is fixed over a certain region of pressure and temperature, the system behaves as if it were a single component system. However, it does not follow that it contains only one chemical species.

In a two component system for example, consisting of one hydrocarbon and water, the phase rule states that with three-phase equilibrium such as hydrate-vapor-water rich liquid, there is only one

degree of freedom. If it is considered that one more hydrocarbon may be introduced into the above system in variable amounts for the same three-phase equilibrium then there would be two degrees of freedom.

This would be represented as a surface on a phase diagram. On the other hand, if the hydrocarbon composition of this three component system is fixed, that is one phase variable has been specified, then only the temperature or the pressure can be varied independently.

Similarly, a multicomponent system in which the hydrocarbon composition is fixed has only one remaining degree of freedom for the three-phase equilibrium hydrate-water rich liquid-hydrocarbon rich liquid.

Figure 1 is a qualitatively representative phase diagram for a system of three components with methane, isobutane and water.

Methane is well above its critical conditions while isobutane is below its critical condition for three phases equilibria (H , L_1 , G). The line $(H_{II}, L_1, G)_B$ is terminated by the quadruple point $(H_{II}, L_1, L_2, G)_B$ with the addition of a new phase, liquid hydrocarbon. Starting from the quadruple point, the four-phase equilibrium line is terminated by the critical locus of methane and isobutane because L_2 becomes identical to G . This four-phase locus can be determined from the intersection of two three-phase equilibrium lines $(H_{II}, L_1, G)_{AB}$ and $(L_1, L_2, G)_{AB}$ as indicated in the diagram or from direct experimental measurements along the H_{II}, L_1, L_2, G locus.

Methane can exist in either hydrate Structure I or II, or both of them. When only hydrate I forming components are present in the system, methane will form hydrate with Structure I. But if there are some hydrate II forming components in the system, methane will form

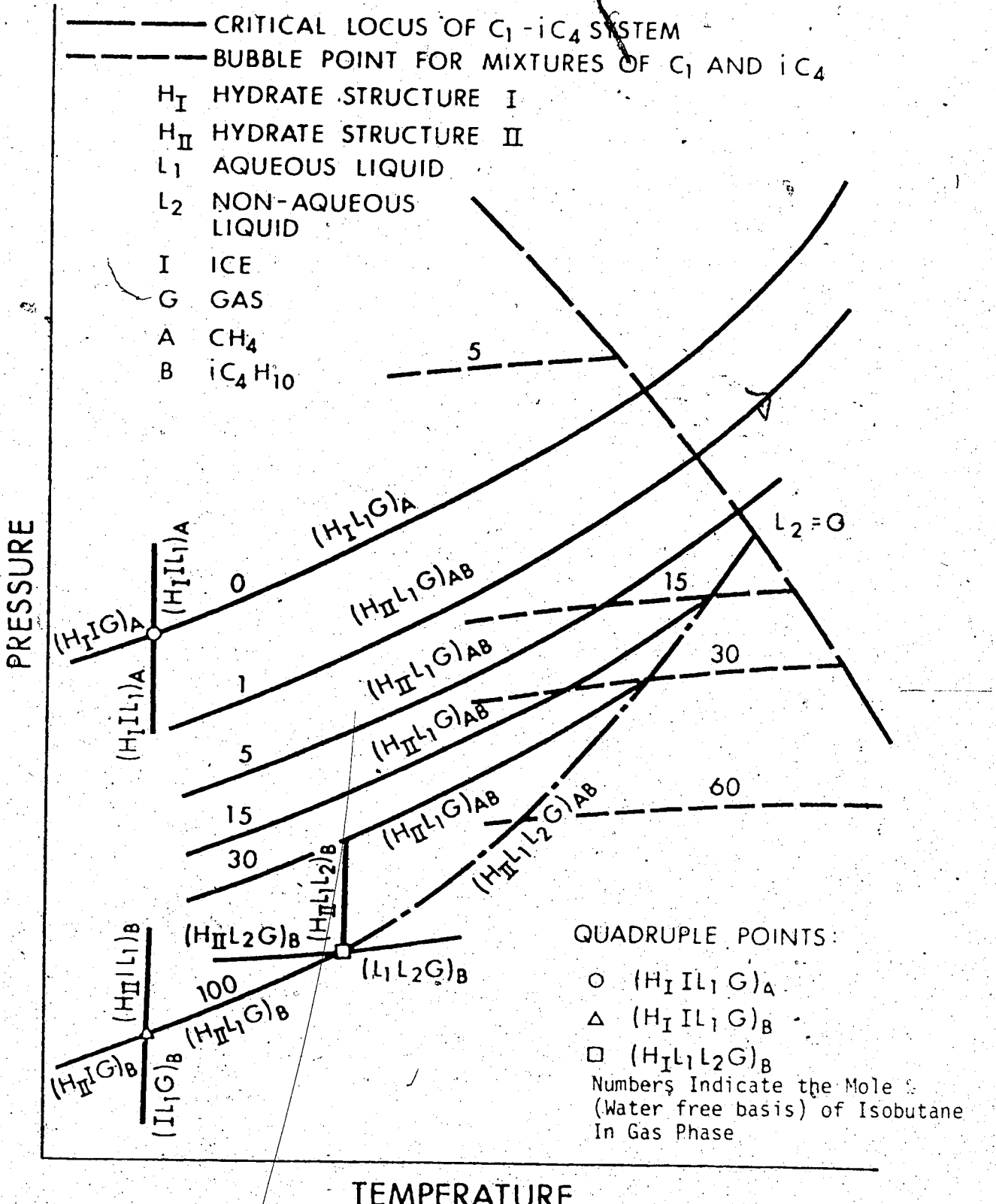


FIG. 1 Qualitative Representation of Phase Behavior of the Ternary System CH_4 - iC_4H_{10} - H_2O for Hydrate Formation

hydrate II. Isobutane can only form in hydrate Structure II and consequently in mixtures of methane and isobutane, only hydrate Structure II exists.

B. Use of Statistical Mechanical Theory in Gas Hydrates Studies

Van der Waals and Platteeuw [9] derived the solid solution theory of gas hydrates from a simple model which corresponds to the three dimensional generalization of ideal localized adsorption by using a grand partition function. They obtained several principal thermodynamic equations for gas hydrates such as the dissociation pressure of the hydrate at various temperatures, the heats of formation of hydrates, and the compositions of the co-existing equilibrium phases.

The basic equations are:

$$= RT \sum_i c_i \ln (1 + \sum_j c_{ij} f_j)$$

where $\Delta \mu^H$ is the difference in chemical potentials of the empty hydrate lattice (μ^0) and the filled hydrate lattice (μ^H), v_i is the number of cavities of hydrate type i per H_2O molecule in the lattice, w_{ik} is the probability of finding a molecule of gas k in a cavity of a hydrate lattice of type i , C_{ik} is the Langmuir constant for molecules of k in cavities i , $w(r)$ is spherical symmetrical potential of molecule k at the distance

r from its centre to the wall of the cavity, and f_j is the fugacity of gas molecules j and is related to y_j , the mole fraction in the gas phase, and p , the total pressure by

Equation (1) is a generalization of Raoult's law which is for the properties of the solvent in a solution where solute-solvent interaction can be neglected. Equation (2) is Langmuir's isotherm for localized adsorption without interaction of the adsorbed molecules.

Van der Waals and Platteeuw [9] considered the gas molecule moving about in a spherical cage formed by the water molecules and applied the Lennard-Jones-Devonshire cell theory. McKoy and Sinaoglu [14], Nagata and Kobayashi [17, 18], and then Parrish and Prausnitz [2] used Kihara potential for the force field in the cavity by consideration of the shape and size of the interacting molecules. The L-J-D cell model with Kihara spherical core potential was modified as

$$(r) = \dots, r \leq 2a$$

$$F(r) = 4 \cdot \left[\left(\frac{r}{r - 2a} \right)^{12} - \left(\frac{r}{r - 2a} \right)^6 \right] \quad r > 2a$$

where ε is the potential minimum, a is the distance parameters where

$r(r) = 0$, and a is the core radius. In this potential model a molecule with a spherical core, e.g., CH_4 , of radius a interacts with a "point molecule". The spherical core molecule represents the solute molecule in the cavity while the point molecule represents the water molecule in the lattice.

Summing all of the gas-H₂O interactions in the cell, we obtain

the cell potential (14)

$$W(r) = 2z \cdot \left[\frac{12}{R^2 r} \left(\frac{10}{r} + \frac{a}{R} \right)^{11} - \frac{6}{R^5 r} \left(\frac{4}{r} + \frac{a}{R} \right)^5 \right] \quad \dots \dots \dots (6)$$

where

$$N = \left[\left(1 - \frac{r}{R} - \frac{a}{R} \right)^{-N} - \left(1 + \frac{r}{R} - \frac{a}{R} \right)^{-N} \right] / N \quad \dots \dots \dots (7)$$

where $N = 4, 5, 10$, or 11 in Equation 6, z is the coordination number and R is the cell radius of the cavity.

Using Equations (1), (2) and (6), we can calculate $\Delta\mu^H$ and then predict hydrate formation conditions, if we know the Kihara parameters and a .

C. Numerical Method for the Prediction of Hydrate Formation Conditions

For a hydrate to exist in equilibrium with the other coexisting phases the chemical potential of each phase should be equal. In the case ice is present,

$$\mu^H(T, P, \dots) = \mu^I(T, P) \quad \dots \dots \dots (8)$$

where $\mu^I(T, P)$ is the chemical potential of ice. If liquid water is present,

$$\mu^H(T, P, \dots) = \mu^L(T, P) + RT \ln x_w \quad \dots \dots \dots (9)$$

where $\mu^L(T, P)$ is the chemical potential of pure liquid water at T and P , and x_w is mole fraction of water in the liquid phase. (x_w is very close to unity for many gases.) When one lets $\Delta\mu^I(T, P) = \mu^E - \mu^I$ or $\Delta\mu^L(T, P) = \mu^E - \mu^L$ and substitutes in Equation (1), then if ice is present

$$\Delta\mu^I(T, P) = RT z \sum_i \ln \left(1 + \sum_j C_{ij} f_j \right) \quad \dots \dots \dots (10)$$

or if liquid water is present,

$$\Delta\mu^L(T, P) = RT z \sum_i \ln \left(1 + \sum_j C_{ij} f_j \right) + RT \ln x_w \quad \dots \dots \dots (11)$$

From Equation (10) or (11), we obtained the calculated potential difference.

In this work fugacity coefficients were calculated by Chueh and Prausnitz's [34] computer program. Gas solubilities were estimated with the Krichevsky and Kasarnovsky equation [35], and the method of Morrison [36].

The chemical potential difference $\mu_L^0 - \mu_L$ or $\mu_L^0 - \mu_L^1$ in Equations (10) or (11) respectively is a function of pressure and temperature only. When hydrate is in equilibrium with the other phases (ice and liquid water) the pressure and temperature effects on this chemical potential therefore become

$$d(\frac{U}{RT}) = -(\frac{\partial H}{RT^2})dT + (\frac{\partial V}{RT})dP$$

where ΔH represents the difference between molar enthalpy and ΔV the difference between the molar volume of the empty hydrate lattice and liquid water.

Integrating Equation (12) along the equilibrium line, it then becomes

$$\frac{(T, P)}{RT} = \frac{(T_0, P_0)}{RT_0} - \int_{T_0}^T \left(\frac{\partial H}{\partial T} \right)^2 dT + \int_{T_0}^T \left(\frac{\partial V}{\partial T} \right) \cdot (dP/dT) dT \quad (13)$$

where dP in Equation (12) is replaced by $(dP/dT)dT$ because the system is univariant, and dP/dT is the slope of the pressure-temperature equilibrium curve.

Using Equation (13), one can calculate the chemical potential difference $\Delta\mu^{\circ}(T, P)$ or $\Delta\mu^L(T, P)$ at the given temperature T and the reference hydrate dissociation pressure P_R for the reference hydrate when either ice or liquid water is present:

If we let temperature be constant and integrate Equation (12) with respect to P_R , we obtain,

The experimental chemical potential difference [$\Delta\mu^{\circ}$ (T, P) or $\Delta\mu_L^{\circ}$ (T, P)] can be calculated by using Equations (13) and (14).

For temperature above 0°C methane and natural gas mixtures [22, 27] were chosen as the reference components for Structure I and Structure II respectively. For temperature below 0°C, xenon and bromochlorodifluoromethane were chosen as the reference hydrates for Structure I and Structure II respectively. Pressure-temperature curves were fitted (2) for reference hydrates by the empirical equation

$$\ln P_R = A_R + B_R/T + C_R \ln T$$

where A_R , B_R , and C_R are constants fitted to represent the experimental data. These constants are given in Table 2.

All the thermodynamic properties needed in Equation (13) and (14) are given in Table 3. V was assumed to be independent of temperature and pressure. For the chemical potential difference between empty hydrate and ice at 0°C and zero pressure, Parrish [2] used the reported value of 211 cal/mol [37] for Structure II. For Structure I, the previous value of 167 cal/mol [9] was doubted by Allen and Jeffrey [38] through their x-ray study of bromine hydrate because bromine hydrate has a tetragonal crystal structure rather than the cubic lattice of Structure I gas hydrates. A value of 302 cal/mol was estimated by Parrish [2]. This value compared well with the value reported by Child [39]. For the gases involved in this investigation, the Kihara parameters for gas-H₂O interaction are listed in Table 4.

CHAPTER 4

EXPERIMENTAL METHODS

A. Experimental Apparatus and Materials

(1) Equipment

The equipment used in this investigation was essentially the same as that used by previous workers [28, 40] except for a newly designed trunnion used for rotating the cell and its contents. Figure 2 shows a schematic diagram of the equipment and piping arrangement.

The equilibrium cell A was designed and fabricated by the Department of Chemical Engineering and was similar to a Penberthy liquid level gauge. It was capable of withstanding 3,500 psia at 100°F. The cell body was constructed from type 316 stainless steel and had an approximate volume of 80 cc. The front and back faces of the cell contained a pyrex window which was manufactured by the Corning Glass Company and was rated at 9,000 psia at 100°F.

The cell A was enclosed in a lucite shell B. The cell and shell were mounted on the trunnion C shown to the right of the main cell.

A detail of the trunnion is given in Figure 3. The cooling fluid was circulated into the space between the lucite shell and the cell through the trunnion and back again to a temperature bath to control the cell temperature. The trunnion was connected to an agitation mechanism driven by a motor and acentric shaft which could be used to rotate the cell and its contents back and forth through an angle of approximately 30 degrees. The cell was connected to the charging and sampling line on the top and to the tubing line going to the Ruska displacement mercury pump D at the bottom of the cell. Mercury was used as the

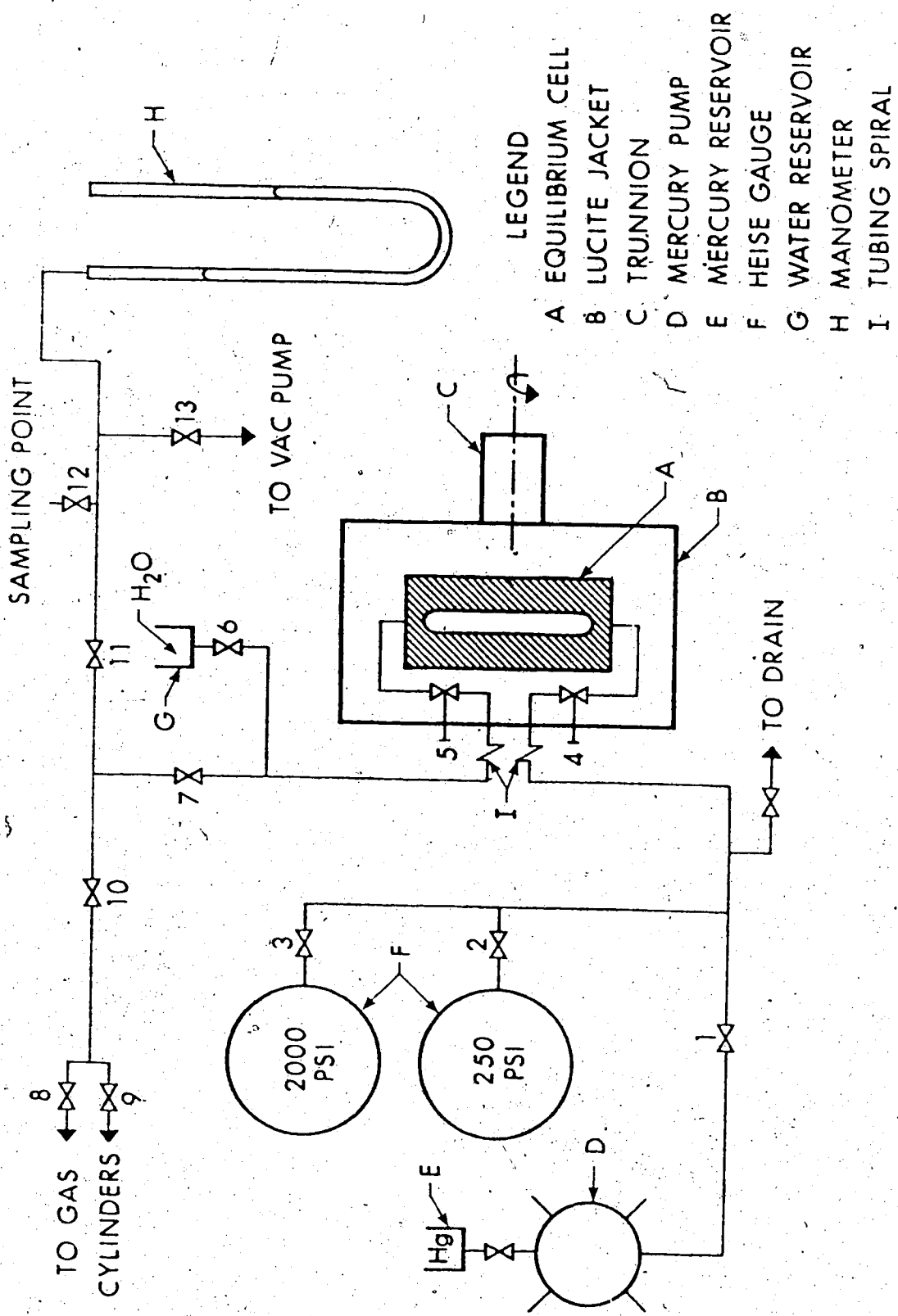


FIG. 2 Schematic Diagram for the Equipment

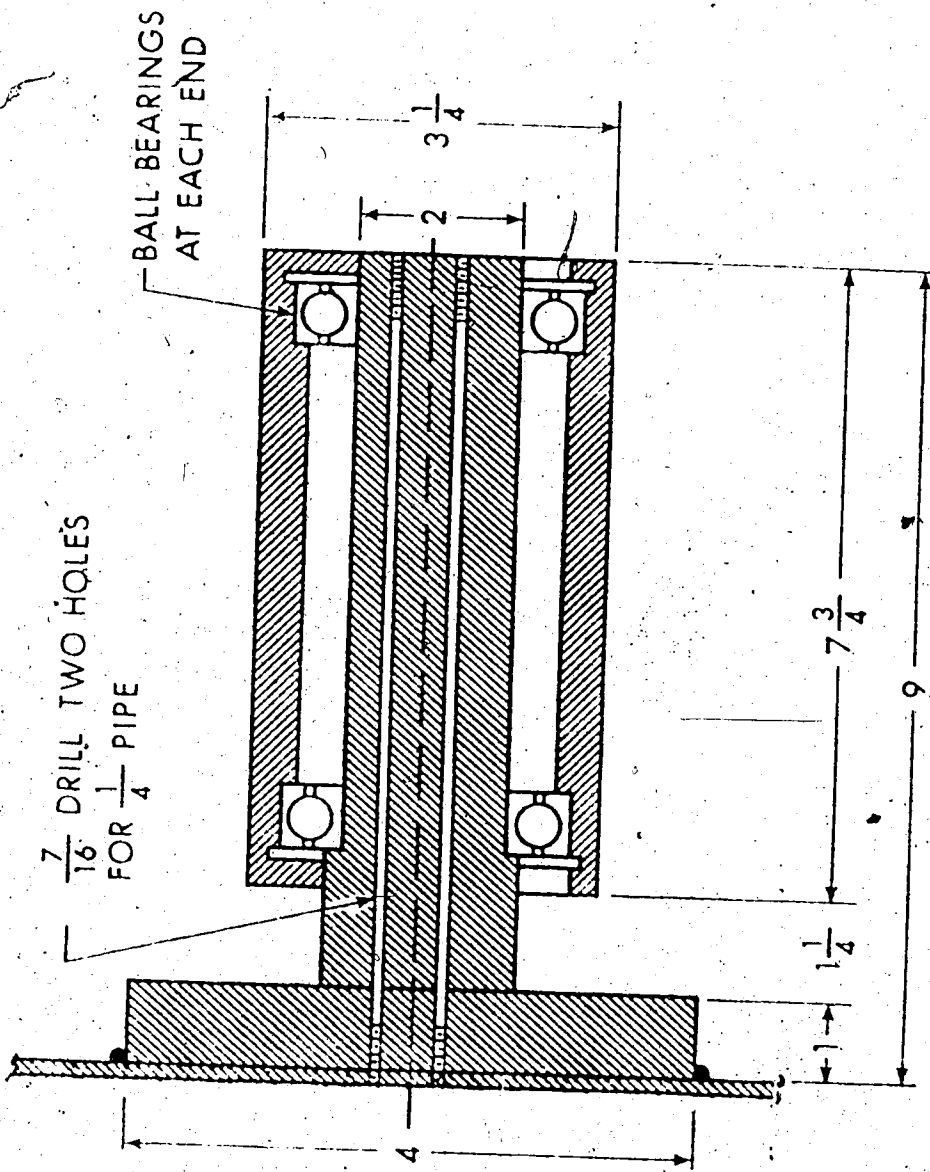


FIG. 3 Schematic Diagram for the Trunnion

confining fluid. The two tubing lines were made from spiral coils of Autoclave high pressure tubing inserted into the lucite shell at the left side. A SWAGELOK quick connection valve which was rated from vacuum to 2,500 psia was used at the sampling point.

(2) Control and Measurement of Temperature

As indicated earlier, the temperature of the equilibrium cell was controlled by circulating a coolant from an auxillary temperature bath through the lucite shell jacketing the cell. Denatured ethanol was used as the circulating fluid. The temperatures inside and outside the cell were measured by two copper-constantant thermocouples and a Leeds-Northrup Model 8686 millivolt potentiometer. The calibration of the thermocouples is shown below:

Temp. (°C)	TC Error (°C)	
	Cell	Bath
0.0	-0.177	-0.058
24.4	-0.157	-0.109
43.25	-0.115	-0.113
97.88	-0.403	-0.445

The temperature was controlled by an American Instrument Company bimetallic strip controller which could be set to govern either the refrigerator or the heater but not both simultaneously. By using this controller, the temperature inside the cell could be controlled to within $\pm 0.1^{\circ}\text{F}$.

(3) Measurement of Pressure

The pressure in the cell was generated by a Ruska Instrument Corporation positive displacement pump with a capacity of 250 cc and

rate at 10,000 psia. Two Heise Bourdon tube gauges rated at 250 psia and 2,000 psia were used for pressure measurement. The gauges were calibrated with a dead weight tester. Corrections for the measured pressure in the cell were made for atmospheric pressure and for the head of mercury between the gauge and the cell. The accuracy of each gauge was within 0.05% of full scale.

(4) Materials

Matheson Incorporated ultra high grade methane and instrument grade propane and isobutane were used. They were certified to be 99.97, 99.5, and 99.5 mole percent chemically pure respectively. The ethane used was Phillips research grade with a reported analysis of 99.94 mole percent ethane. The analyses were confirmed by the fact that no detectable impurity peaks were observed during the chromatographic analyses of the samples.

B. Experimental Techniques

(1) Preparation of Mixtures

Initially all the system was evacuated, flushed with the testing gas, and re-evacuated. Valve 7 was closed and approximately 10-15 cc of distilled water were introduced into the cell. Valves 11 and 6 were closed, valve 10 was opened, and the predetermined amount of each gas was charged into the cell. The amount was based on the pressure reading observed on the proper Heise gauge. In making a mixture, the gas from the lower pressure tank was introduced first. With valve 5 closed, the cell was continuously rocked for approximately 30 minutes

to ensure that the gases were thoroughly mixed. A sample of the mixture was then taken for analysis.

When a condensed liquid sample was being prepared, it was found necessary to take several samples before consistent reproducible analyses were obtained. This was so because the contents of the lead lines could not be thoroughly mixed with the cell contents.

(2) Hydrate Formation

The cell temperature was lowered to 10-15°F below the estimated hydrated formation condition. More agitation of the cell caused the hydrate to form. When this had happened, the temperature was increased slowly until the hydrate began to melt. The temperature was kept at 0.3-3°F higher than the melting point to let almost all of the hydrate dissociate. The temperature was then lowered by 0.5-3°F to recrystallize the hydrate. A few crystals of hydrate that remained on the glass window served as seed crystals for the hydrate formation. The temperature was raised again very slowly until the hydrate on the window just began to melt. Hydrate dissociation was always also accompanied by a sharp rise in pressure. The temperature and pressure were recorded at this point. The physical phenomenon of hydrate formation in the liquid phase resembles that in the gas phase. However, when the temperature was increased very slowly to the equilibrium point at a condition close to the bubble point in mixtures containing a relatively high concentration of methane, many bubbles developed in the liquid water phase no matter how carefully the procedure had been followed.

(3) Gas Chromatographic Analysis

Sample analysis was accomplished by using a Hewlett-Packard Model 5750B gas chromatograph. Porapak Q columns were used with column length of three and six feet. The thermal conductivity cell was maintained at 120°C and 65°C, with 150 ma current and a Helium flow rate of 20 cc/min. The sample size was measured with a differential pressure transducer. The gas chromatograph was connected directly on-line with the Department IBM 1800 computer which permitted fast convenient data processing and digital filtering of data. The Chromatograph Monitoring Program was used to standardize each component investigated in the analysis to obtain the proper corresponding response factor, and to analyze the results of the samples. The smooth standardization curves are shown in Figure 4. By using the Chromatograph Monitoring Program analyses were reproducible to within $\pm 0.3\%$.

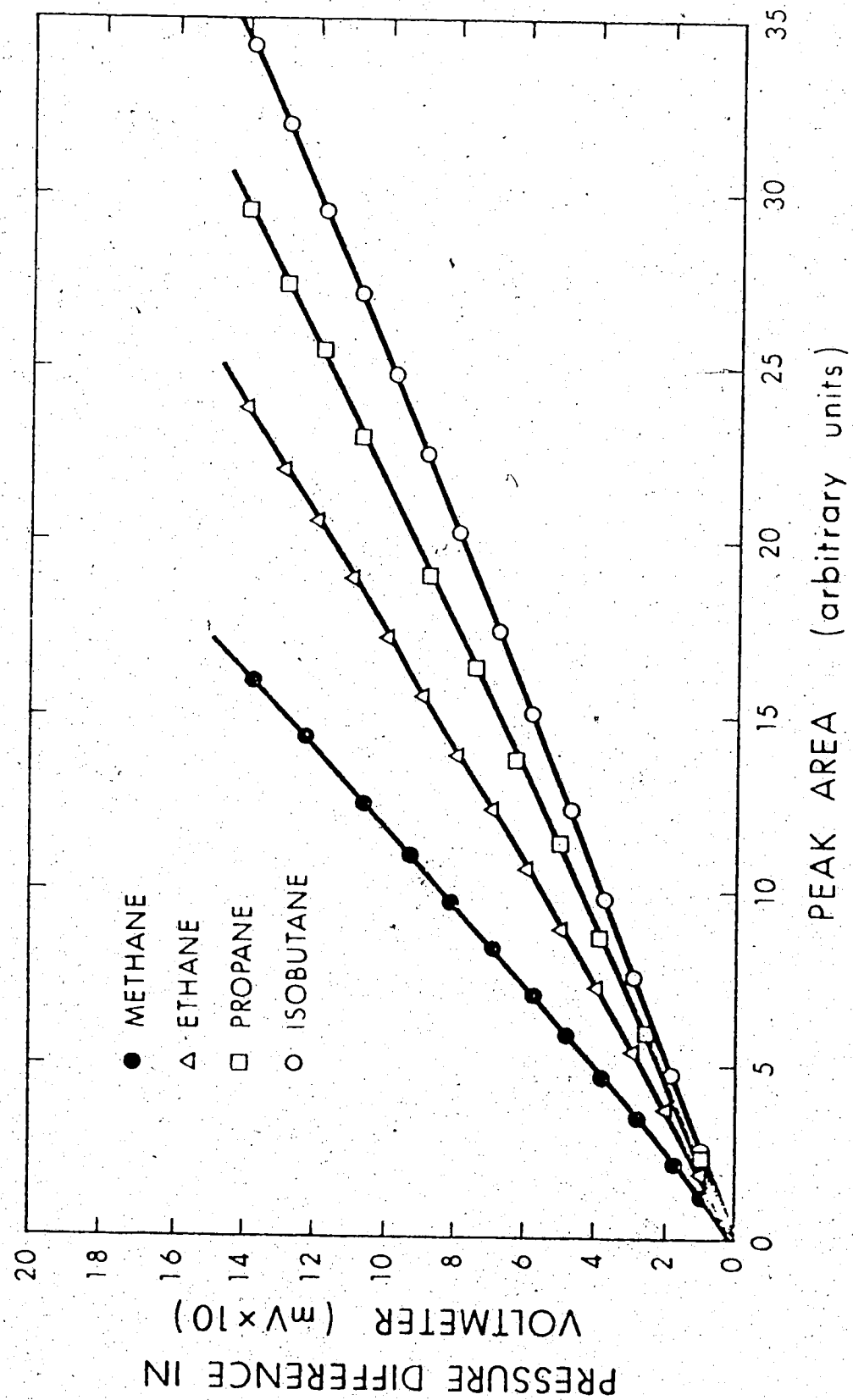


FIG. 4 Gas Chromatograph Standardization

CHAPTER 5

EXPERIMENTAL RESULTS

A. Methane-Isobutane-Water System.

The experimental results for the different compositions of the methane-isobutane gas mixtures in the three-phase equilibrium (H, L, G) are given in Table 5. The results are plotted in Figure 5. In order to verify the experimental technique the binary system consisting of pure methane and water was tested. Good agreement between this work and that of other investigators [19; 20, 21, 22, 23, 24] was obtained.

The experimental data of those authors and this investigation are given in Table 6 and depicted in Figure 5. For isobutane hydrate Rouher and Barduhn's data are tabulated in Table 7 and depicted in Figure 5. The experimental data of Deaton and Frost [21] and McLennan and Campbell [27] for several methane-isobutane mixtures are given in Table 8.

B. Hydrates of Liquefied Light Hydrocarbon

Mixtures

Initial hydrate formation conditions for the L₁-L₂-H equilibrium for these liquefied hydrocarbon gas mixtures were determined. The composition of the mixtures and the experimental results are listed in Table 9 and Table 10. Smooth curves have been drawn through the experimental points shown in Figure 6. The bubble point lines in the figure were predicted using a computer program based on the Chueh-Prausnitz correlation. It was an interesting and significant discovery to note that when the concentration of methane in the liquefied mixtures increased, the pressure had more effect on the hydrate formation.

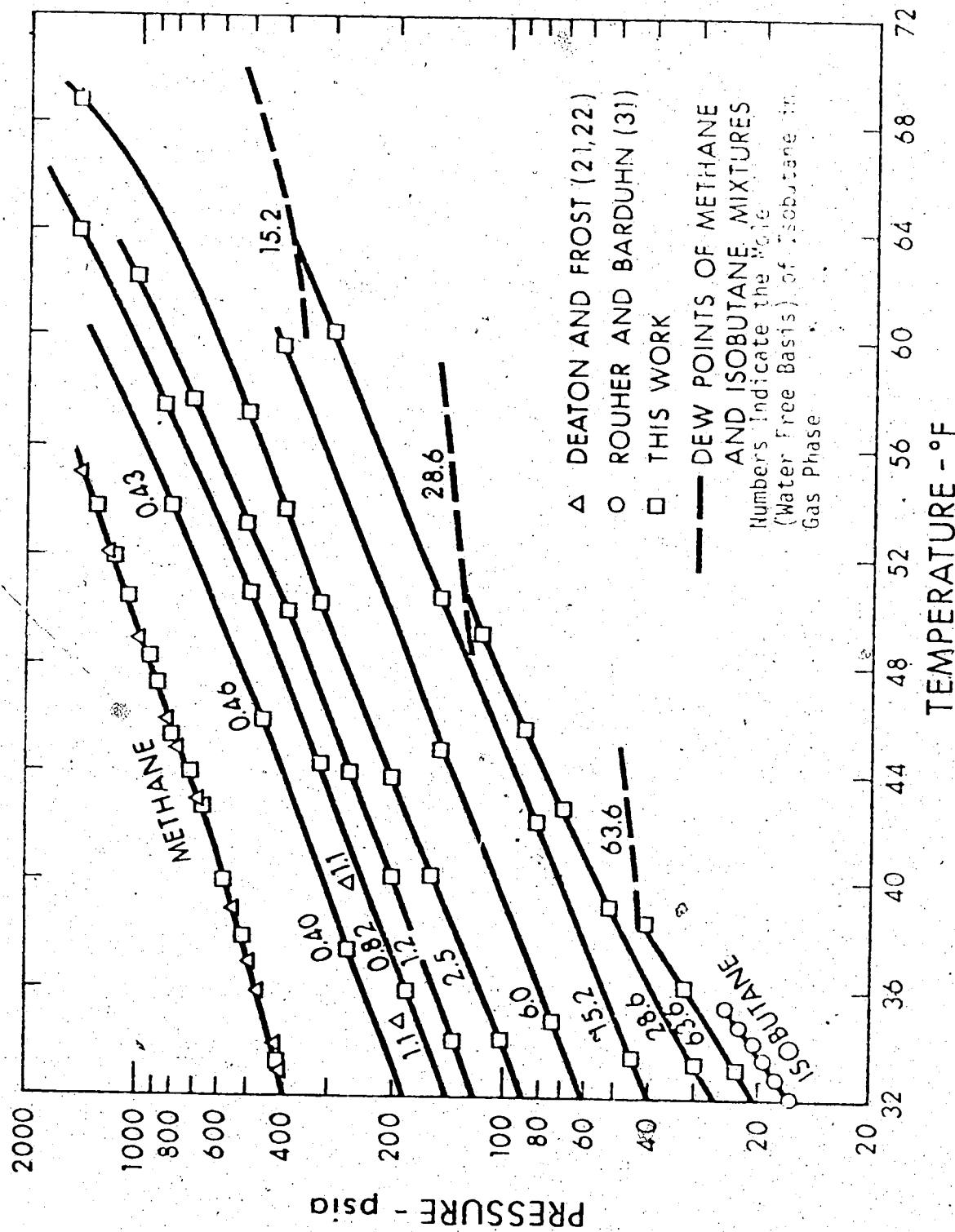


FIG. 5 Conditions for the Ternary $\text{CH}_4\text{-C}_4\text{H}_{10}\text{-H}_2\text{O}$ System in $\text{H}_2\text{-O}_2$ Phase Equilibrium

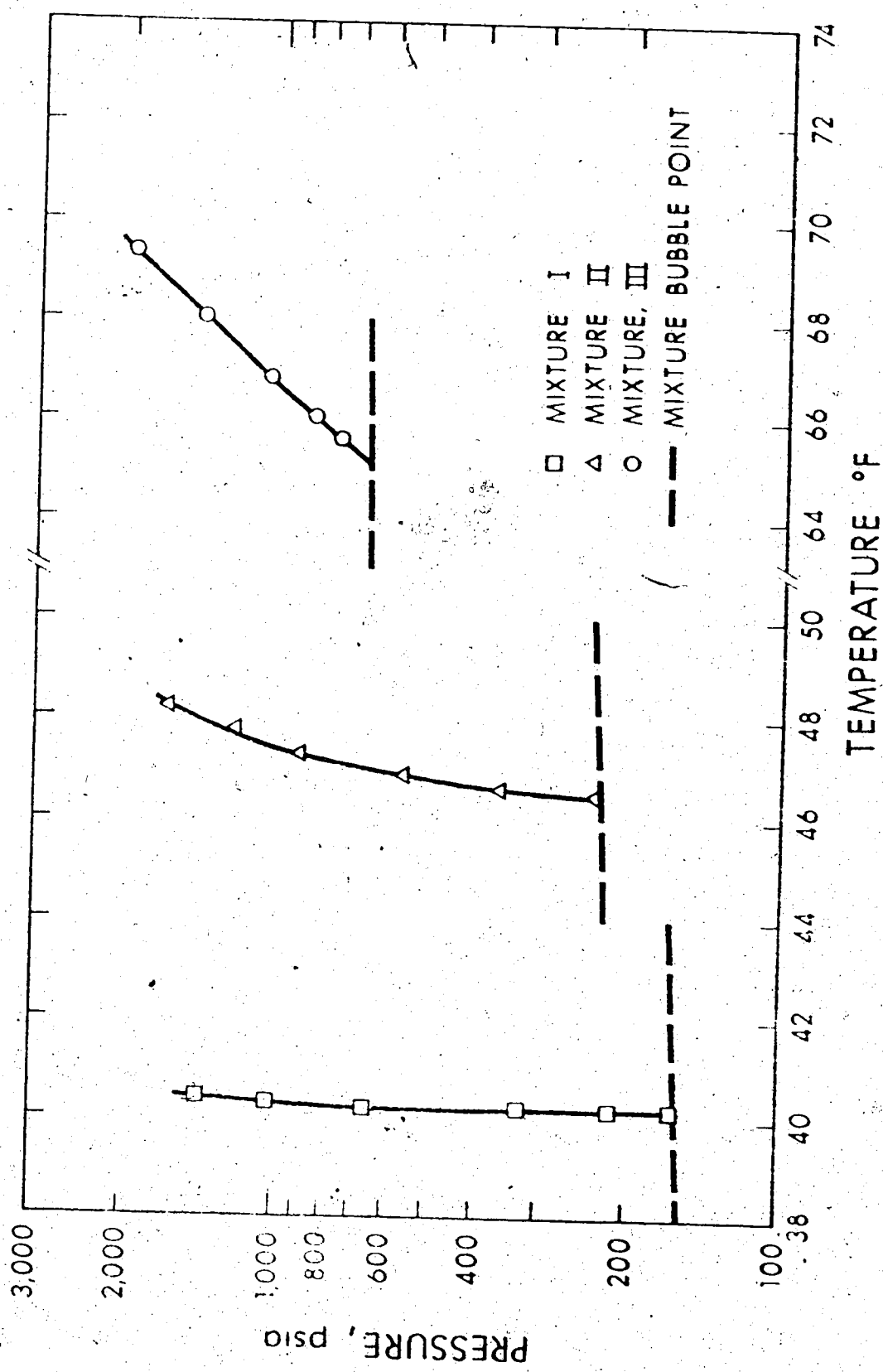


Fig. 6. Conditions for the Liquefied Light Hydrocarbon Mixtures in $L_1-L_2-H_2$ Equilibrium

, temperature. Mixture I, containing no methane, has a nearly vertical equilibrium curve up to 1,000 psia.

CHAPTER 6

THEORETICAL RESULTS

A computer program based on the numerical procedure proposed by Parrish and Prausnitz [2] was written. The detailed procedure was described in Chapter 3, Section C. This program is given in Appendix C. At a later date, and through correspondence with Professor Prausnitz a copy of the program which had been used in the original paper was obtained. Both programs were used in carrying out the theoretical calculations.

A. Hydrate Formation Prediction for Methane-Isobutane-Water System

Predicted results compared with experimental data for methane and isobutane mixtures are given in Table 11. The program predicts well for higher mole percent isobutane mixtures but not so well for lower concentrations. No gas solubility data are available for isobutane in water in the literature. In preparing the program, it was assumed that the gas solubility of isobutane is approximately the same as that of n-butane. The gas solubility data obtained by Morrison [36] for methane and n-butane in water was used for the predictions of the methane-isobutane mixtures.

B. Hydrate Formation Prediction for Liquefied Hydrocarbon Gas Mixtures

At the hydrocarbon bubble point, it should be possible to predict initial hydrate formation conditions in the liquid system because the vapour phase exists and is in equilibrium with liquid phase and hydrate phase. The hydrate formation equilibrium line in the liquefied phase

is extended to intersect the bubble point locus. The quadruple points (L_1 , L_2 , H,G) were located in Figure 6. The composition in the vapour phase at the bubble point was used to predict hydrate formation conditions. A comparison between experimental and calculated hydrate formation conditions is given in Table 12. The program predicted the hydrate formation condition reasonably well with a maximum deviation in temperature of -2.8°F . In a liquefied light hydrocarbon mixture containing a lower concentration of methane, the hydrate formation condition in the liquid mixture can be estimated without serious error.

CHAPTER 7

DISCUSSIONS AND CONCLUSIONS

A. Validity of Experimental Data

Temperature measurements were accurate to within $\pm 0.1^\circ\text{F}$. Pressure could be determined to accuracies of $\pm 1.0 \text{ psi}$ with the 2,000 psi Heise gauge and $\pm 0.125 \text{ psia}$ with the 250 psi Heise gauge. By using the Chromatograph Monitoring Program, the sample analyses were determined with an accuracy with $\pm 0.3\%$. For the lower mole percent isobutane mixtures a Hewlett-Packard Model 17503A Recorder was used. The analyses were reproducible to within $\pm 0.02\%$.

B. Methane-Isobutane-Water System

From the theoretical model we find the composition in the hydrate lattice is different from that in the gas phase. Therefore, the amount of hydrate remaining in the cell will effect the gas phase composition and consequently change the hydrate formation condition. It becomes very important to allow only a few hydrate crystals to exist when the point of incipient hydrate formation is recorded. In this way, the gas phase composition will keep approximately constant at different conditions for each mixture. For lower concentrations of isobutane, the effect of the amount of hydrate existing becomes even more significant. It was found necessary to analyse the vapour phase composition for each different condition.

The data obtained by Deaton and Frost [21] deviate considerably from this investigation. One of the reasons for the deviation might be that the equilibrium gas phase concentration of isobutane in Deaton and

Frost's work was actually somewhat less than that in the original mixture composition of 1.1 mole %. Another reason could possibly be errors in the analysis of the gas mixture.

C. Liquid Hydrocarbon Mixtures

From the experimental results it was found that methane has a significant effect on the nature of hydrate formation for a liquid hydrocarbon mixture. In other words, in a mixture containing a relatively low concentration of methane, the hydrate equilibrium line in the liquid region will be nearly vertical. Therefore, if we can predict hydrate formation condition at the bubble point, we can estimate the hydrate formation at higher pressure for liquid mixtures without serious error. The experimental results confirmed the fact that the theoretical prediction method could also be used for liquid hydrate formation. A maximum temperature deviation of -2.8°F . was found for a mixture containing methane, ethane, propane and isobutane.

D. Conclusion

The study of hydrate of the methane-isobutane-water system has contributed to the available data on natural gas hydrate forming systems. Isobutane has been shown to exert a considerable influence on initial hydrate formation condition even when it is present in a concentration as low as 0.4 mole%.

The investigation of hydrate formation in liquefied light hydrocarbon mixtures verified that the theoretical prediction method could be used for representative mixtures containing variable amounts of methane, ethane, propane and isobutane.

CHAPTER 8FUTURE WORK

1. The determination of the effect of carbon dioxide, hydrogen sulfide, and some of the non-hydrate forming heavier hydrocarbons on the L₁-L₂-H equilibrium.
2. The completion of a computer program to predict hydrate formation at the bubble point for liquid mixtures by combining the hydrate formation prediction program with the bubble point prediction program.

NOMENCLATURE

a	Core radius, Å
A_R, B_R, C_R	Fitted constants for calculating dissociation pressure of a reference hydrate
C	Number of components
C_{ik}	Langmuir constant for components k in cavity i
F	Number of degrees of freedom
f_j	Fugacity of component j
H	Hydrate phase
H_I	Hydrate phase with Structure I
H_{II}	Hydrate phase with Structure II
h	Molar enthalpy, cal/mole
G	Gas phase
k	Boltzmann's constant, 1.38×10^{-6} erg/°K
L_1	Liquid water rich phase
L_2	Liquid hydrocarbon rich phase
M	Number of hydrate forming molecules
M_1	Number of hydrate forming molecules in smaller cavities of Structure I
M_2	Number of hydrate forming molecules in larger cavities of Structure I
M_3	Number of hydrate forming molecules in smaller cavities of Structure II
M_4	Number of hydrate forming molecules in larger cavities of Structure II
N	Integer constant in Equation (7)
n	Number of "host" water molecules
p	Total pressure, atm

P_0	Dissociation pressure at ice point, atm
P_R	Dissociation pressure of reference hydrate, atm
r	Radial coordinate Å
R	Gas constant, 1.987 cal/mole°K; cell radius, Å
T	Temperature, °K
T_0	Temperature at ice point, 273.15°K
V	Molar volume, cc/mole
$w(r)$	Spherically-symmetric cell potential, ergs
x_w	Mole fraction of liquid water
y_j	Mole fraction of component j in gas phase
z_m	Coordination number of cavity type m

Greek Letters

$\tau(r)$	Kihara potential, ergs
δ	Polynomial defined by Equation (7)
ϵ	Depth of intermolecular potential well, erg
θ_{ij}	Fraction of cavities type i occupied by component j
μ	Chemical potential, cal/mole
n_i	Number of cavities type i per water molecule in the hydrate
a_i	Distance parameter, point at which $\tau(r) = 0$, Å
ϕ_j	Fugacity coefficient

Superscripts

o	Property at ice point
H	Hydrate phase

L Liquid water phase

R Reference hydrate

a Ice phase

B Empty hydrate phase

Subscripts

j, k Component

i Cavity type i

BIBLIOGRAPHY

- [1] Hammerschmidt, E. G., Ind. Eng. Chem., 26, 851 (1934).
- [2] Parrish, W. R., Prausnitz, J. M., I & EC Process Des. Develop., 11, No. 1, 26 (1972).
- [3] Stackelberg, M., Müller, H. G., J. Chem. Phys., 19, 1319 (1951).
- [4] Müller, H. G., Stackelberg, M., Naturwiss., 39, 20 (1952).
- [5] Claussen, W. F., J. Chem. Phys., 19, 259 (1951).
- [6] Claussen, W.F., J. Chem. Phys., 19, 1425 (1951).
- [7] Pauling, L., Marsh, R. E., Proc. Nat. Acad. Sci., U. S. A. 38, 112 (1952).
- [8] Jeffrey, G. A., McMullan, R. R., Progr. Inorg. Chem., 8, 43 (1967).
- [9] Van der Waals, J. H., Platteeuw, J. C., "Advances in Chemical Physics", 2, 1 (1959), Interscience, New York.
- [10] Byk, S. S., Fomina, V. I., Russ. Chim. Rev., 37 (6), 469 (1968).
- [11] Carson, D. B., Katz, D. L., Trans. A.I.M.E., 146, 150 (1941).
- [12] Wilcox, W. I., Carson, D. B., Katz, D. L., Ind. and Eng. Chem., 33, 662 (1941).
- [13] Natural Gas Processors Suppliers Association, "Engineering Data Book", 9th ed., Tulsa, Okla., 1972.
- [14] McKoy, V., Sinanoglu, O., J. Chem. Phys., 38, 2946 (1963).
- [15] Saito, S. H., Marshall, D. R., Kobayashi, R., A.I.Ch.E. J., 10, 734 (1964).
- [16] Saito, S. H., Kobayashi, R., A.I.Ch.E. J., 11, 96 (1965).
- [17] Nagata, I., Kobayashi, R., Ind. Eng. Chem. Fundamentals, 5, 344 (1966).
- [18] Nagata, I., Kobayashi, R., Ind. Eng. Chem. Fundamentals, 5, 466 (1966).
- [19] Villard, P., Compt. Rend., 106, 1602 (1888).
- [20] Ibid., 107, 395 (1888).
- [21] Beaton, W. M., Frost, E. M., Gas 16, No. 6, 28-30, (1940).

- [22] Deaton, W. M., Frost, E. M., Oil and Gas J., 45, 170 (1946-47).
- [23] Roberts, O. L., Brownscombe, E. R., Howe, L. S., Oil and Gas J., 39, No. 30, 37 (1940).
- [24] Roberts, O. L., Brownscombe, E. R., Howe, L. S., Ramser, Petrol. Eng., 12, No. 6, 56 (1941).
- [25] Kobayashi, R., Katz, D. L., Trans. A.I.M.E., 186, 66 (1949).
- [26] Kobayashi, R., Katz, D. L., J. Petrol. Technol., 1, No. 3, 66 (1949).
- [27] Campbell, J. M., McLeod, H. O., Trans. A.I.M.E., 222, 590 (1961).
- [28] Otto, F. D., Robinson, D. B., A.I.Ch.E. J., 6, 602 (1960).
- [29] Marshall, D. R., Saito, S. H., Kobayashi, R., A.I.Ch.E. J., 10, 22 (1964).
- [30] Kayano, I., Utida, T., J. Chem. Soc. Japan, Ind. Chem. Sect., 67, 997A, 61 (1964).
- [31] Rouher, O. S., Barduhn, A. J., Desalination, 6, 57 (1969).
- [32] Gibbs, J. W., Collected Works, Longmans, 1928, Vol. I, p.p. 55-150, from Trans. Connecticut Acad., 1874-78.
- [33] Von Stackelberg, M., Müller, H. R., Z. Elektrochem., 58, 25 (1954).
- [34] Chueh, P. L., Prausnitz, J. M., Ind. Eng. Chem., Fundam. 6, 492 (1967).
- [35] Prausnitz, J. M., "Molecular Thermodynamics of Fluid-Phase Equilibria", Prentice-Hall, Inc., Englewood Cliffs, N.J., 1969, p. 356.
- [36] Morrison, T. J., J. Chem. Soc. (London), 1952, 3814.
- [37] Sortland, L. D., Robinson, D. B., Can. J. Chem. Eng., 42, 38 (1964).
- [38] Allen, K. W., Jeffrey, G. A., J. Chem. Phys., 38, 2304 (1963).
- [39] Child, W. C., J. Phys. Chem., 68, 1834 (1964).
- [40] Snell, E., M.Sc. Thesis, University of Alberta (1961).

APPENDIX A

DATA PERTAINING TO HYDRATE PHYSICAL
AND MOLECULAR STRUCTURE

TABLE 1
PHYSICAL PROPERTIES OF HYDRATE LATTICE (32)

	<u>Structure I</u>		<u>Structure II</u>	
No. of water molecules/ unit cell	46		136	
	<u>Small</u>	<u>Large</u>	<u>Small</u>	<u>Large</u>
No. of cavities/unit cell	2	6	16	8
Cell diameter, Å (9)	7.95	8.60	7.82	9.46
Corrdination no.	20	24	20	28

TABLE 2
CONSTANTS FOR CALCULATING DISSOCIATION
PRESSURES OF REFERENCE HYDRATES (2)

(P_R is in atmospheres and T is in °K)

	<u>A_R</u>	<u>B_R</u>	<u>C_R</u>	<u>Temperature Range, °K</u>
<u>Structure I</u>				
Xenon	23.0439	-3357.57	-1.85000	211-273
Methane	-1212.2	44344.0	187.719	273-300
<u>Structure II</u>				
Bromochloro-				
difluoromethane	11.5115	4092.37	0.316033	253-273
Natural Gas Mixture	-1023.4	34984.3	159.923	273-291
Natural Gas Mixture	4071.64	-193428.8	-599.755	291-313

TABLE 3

THERMODYNAMIC PROPERTIES OF EMPTY HYDRATE (- Phase)
AND LIQUID WATER RELATIVE TO ICE (.- Phase)
AT 0°C AND ZERO PRESSURE (2)

	<u>Structure I</u>	<u>Structure II</u>
$\mu_w^0 - \mu_w^x$, cal/mole	302	211
$H_w^0 - H_w^x$, cal/mole	275	193
$v_w^0 - v_w^x$, cm^3/mole	3.0	3.4
$H_w^L - H_w^x$, cal/mole	1436.3	
$C_p^L - C_p^x$, cal/mole		9.11 - 0.0336 ($T - 273.1$)

TABLE 4

KIHARA PARAMETERS FOR HYDRATE-GAS INTERACTIONS (2)

Gas	<u>2a, Å</u>	<u>b, Å</u>	<u>c/K, °K</u>
Methane	0.600	3.2398	153.17
Ethane	0.800	3.2941	174.97
Propane	1.360	3.3030	200.94
Isobutane	1.600	3.1244	220.52
Nitrogen	0.700	3.6142	127.95

40

APPENDIX B

~~EXPERIMENTAL AND PUBLISHED DATA~~

TABLE 5

EXPERIMENTAL DATA FOR METHANE-ISOBUTANE MIXTURES -
HYDRATE FORMATION IN HL/G EQUILIBRIUM

Composition (Mole % of i-C ₄)	psia	°F
0.40	262	37.5
0.43	811	53.8
0.46	457	46.0
0.82	184	36.0
	317	44.4
	485	50.6
	855	57.6
	1,456	63.9
1.2	137.5	34.2
	201	40.2
	261	44.1
	391	50.0
	503	53.2
	707	57.8
	1,008	62.3
2.5	101.6	34.3
	157.3	40.3
	201	43.9
	312	50.3
	398	53.7
	501	57.3
	662	61.0
	1,460	68.8
6.0	73.3	34.9
	147.0	45.0
	245	52.5
	409	59.8
15.2	44.1	33.6
	81.8	42.3
	149.7	50.5
	295	60.3
28.6	29.7	33.4
	51.7	39.2
	69.2	42.8
	87.3	45.7
	114.1	49.2

TABLE 5 - continued

Composition (Mole % of i-C ₄)	psia	°F
63.6	23.0	33.2
	32.0	36.2
	41.1	38.8

TABLE 6

COMPARISON OF METHANE HYDRATE FORMATION CONDITIONS ($\text{H}_\text{L}\text{G}$)
OF THE PUBLISHED DATA AND THIS WORK

<u>Villard (19, 20)</u>		<u>Deaton and Frost (21, 22)</u>		<u>Roberts et al (23, 24)</u>		<u>This Work</u>	
<u>psia</u>	<u>°F</u>	<u>psia</u>	<u>°F</u>	<u>psia</u>	<u>°F</u>	<u>psia</u>	<u>°F</u>
390	32.0	401	33.0	383	32.0	408	33.4
441	34.0	421	34.0	848	46.0	509	38.0
690	41.9	470	36.0	1,452	56.0	578	40.1
934	47.3	496	37.0	1,567	56.4	668	42.8
1,102	49.8	553	39.0			713	44.1
1,220	51.4	692	43.0			794	45.4
1,813	57.7	776	45.0			874	47.3
2,235	61.0	828	46.0			926	48.3
2,650	63.1	879	47.0			1,050	50.5
3,410	66.7	982	49.0			1,150	51.9
3,900	68.5	1,178	52.0			1,293	53.8
		1,419	55.0			1,465	56.0

TABLE 7

PUBLISHED EXPERIMENTAL DATA OF ISOBUTANE-
HYDRATE FORMATION CONDITIONS
IN HL₁G EQUILIBRIUM (30)

psia	°F
16.7	32.1
17.9	32.8
19.5	33.5
20.8	34.1
22.8	34.7
24.4	35.4

TABLE 8

PUBLISHED EXPERIMENTAL DATA OF METHANE-ISOBUTANE
HYDRATE FORMATION CONDITIONS
IN HL/G EQUILIBRIUM

Authors	Composition (mole %)	psia	°F
Deaton and Frost (20)	1.1 (in i-C ₄)	192 267	35.0 40.0
McLeod and Campbell (27)	1.4	985 3055 4875 5005 6915 7125 9025	59.8 71.7 76.0 76.4 80.3 80.1 84.4
	4.6	975 975 1115 1535 2015 2025 2025 3375 3455 5015 7015 7115 9185	70.0 69.2 70.6 71.9 74.0 74.3 75.0 77.0 77.3 81.2 84.9 85.1 89.3

TABLE 9
COMPOSITION OF LIQUEFIED HYDROCARBON MIXTURES
(mol %)

	<u>Liquids</u>		
	I	II	III
Nitrogen	0.25	0.24	0.21
Methane	-	2.23	21.94
Ethane	31.32	30.63	24.67
Propane	51.53	50.73	40.76
i-Butane	16.90	16.17	12.42

TABLE 10
EXPERIMENTAL HYDRATE FORMATION CONDITIONS FOR
FOR THREE LIQUEFIED MIXTURES

<u>Mixture I</u>	<u>Mixture II</u>		<u>Mixture III</u>	
	<u>psia</u>	<u>°F</u>	<u>psia</u>	<u>°F</u>
172	40.2		235	46.5
212	40.2		357	46.6
324	40.2		553	46.9
656	40.2		885	47.3
1,026	40.3		1,194	47.8
1,409	40.4		8	48.2

TABLE 11

 PREDICTED HYDRATE FORMATION CONDITIONS
 FOR METHANE-ISOBUTANE MIXTURES
 IN H_2 - G EQUILIBRIUM

Composition mole % of i-C ₄	Rarrish and Prausnitz's Program (2) °F	Rarrish and Prausnitz's Program (2) psia	This Work psia	Experiment psia
0.40	37.5	323	325	262.0
0.43	53.8	975	951	811.0
0.46	46.0	544	542	457.0
0.82	36.0	229	230	184.0
	44.4	400	399	317.0
	50.6	616	609	485.0
	57.6	1,063	1,019	855.0
	63.9	1,915	1,714	1,456.0
1.2	34.2	175.0	176.0	137.5
	40.2	260	261	201.1
	44.1	338	338	261.0
	50.0	509	502	391.0
	53.2	642	628	503.0
	57.8	923	883	707.0
	62.3	1,388	1,274	1,008.0
2.5	34.3	129.1	129.7	101.6
	40.3	193.7	193.5	157.3
	43.9	247	246	201.0
	50.3	382	376	312.0
	53.7	487	473	398.0
	57.3	636	608	501.0
	61.0	858	797	662.0
	68.8	1,936	1,417	1,460.0
6.0	34.9	90.4	90.5	73.3
	45.0	182.6	180.4	147.0
	52.5	306	297	245.0
	59.8	519	483	409.0
15.2	33.6	52.2	52.2	44.1
	42.3	100.7	99.5	81.8
	50.5	181.9	176.0	149.7
	60.3	370	339	295.0

TABLE 11 - continued

Composition mole % of i-C ₄	°F	Parrish and Prausnitz's Program (2) psia	This Work psia	Experiment psia
28.6	33.4	37.0	37.0	29.7
	39.2	60.0	59.4	51.7
	42.8	80.0	78.7	69.2
	45.7	100.3	98.0	87.3
	49.2	131.1	126.7	114.1
63.6	33.2	23.8	23.7	23.0
	36.2	32.2	31.9	32.0
	38.8	41.6	41.0	41.1

TABLE 12

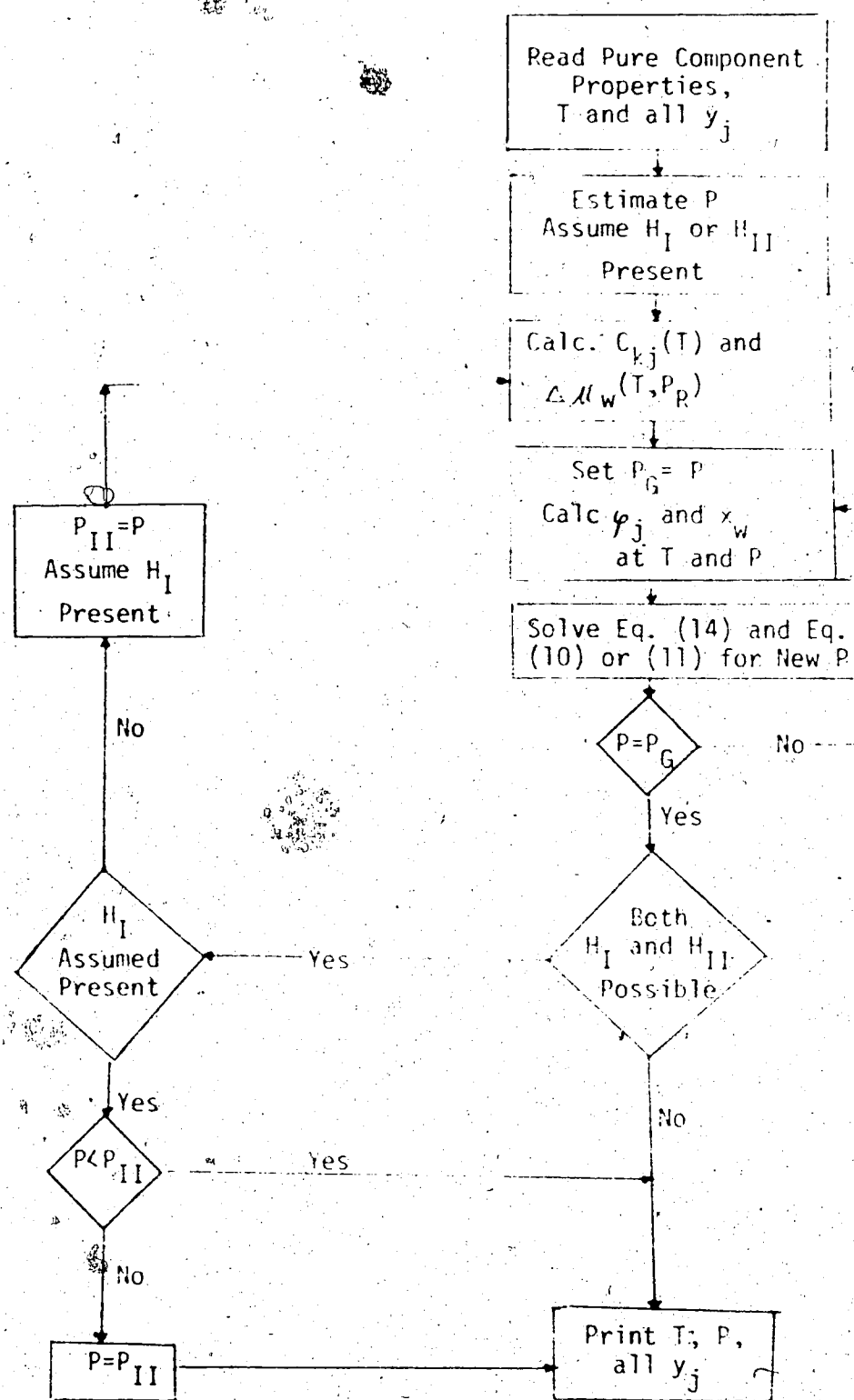
COMPARISON BETWEEN EXPERIMENTAL AND
CALCULATED HYDRATE - FORMATION CONDITIONS
AT BUBBLE POINTS FOR LIQUID MIXTURES

<u>Liquid Mixture</u>	<u>Experimental</u> psia	<u>°F</u>	<u>Calculated</u> psia	<u>°F</u>	<u>Deviation of Temperature, °F</u>
I	169	40.4	157	37.6	-2.8
II	227	46.5	224	45.0	-1.5
III	667	65.1	659	63.0	-2.1

APPENDIX C

COMPUTER PROGRAM FOR GAS HYDRATE
FORMATION PREDICTION

Flow Chart of Computer Program




```

1 CORIJ(I,I),SA(I),SB(I),SC(I)
  WRITE(6,114) PC(I),VC(I),TC(I),A(I),C1FKV(I),C2RKV(I),
1 CORIJ(I,I),SA(I),SB(I),SC(I)
  IF(NCOMP-I) 7,8,7
7  II=I+1
  DO 1 J=II,NCOMP
    READ(5,104) CORIJ(I,J)
    WRITE(6,104) CORIJ(I,J)
1  CONTINUE
8  CONTINUE
  DO 2 I=1,NCOMP
    DO 2 J=1,2
      READ(5,103) ALI(I,J),BLI(I,J)
      READ(5,103) ALII(I,J),BLII(I,J)
      WRITE(6,103) ALI(I,J),BLI(I,J),ALII(I,J),BLII(I,J)
2  CONTINUE
  TF=273.15
  H=-2616.398
  DAH=20.616E
  DBH=-0.0211634
  DELVF=0.0387
  UI(1)=1./23.
  UI(2)=3./23.
  UII(1)=2./17.
  UII(2)=1./17.
10  READ(5,102),TF
  IF(TF).LE.1001.11
11  READ(5,105) (Y(I),I=1,NCOMP)
  WRITE(6,105) (Y(I),I=1,NCOMP)
  DO 333 I=1,NCOMP
    TEMPY(I)=Y(I)
333  CONTINUE
999  HI=0.0
  HII=0.0
  NOL=0.
  ITER=1
  TR=TF+459.69
  TK=TR/1.8
C
C   CALCULATE THE PARTIAL MCLAR VOLUME OF GASES IN THE WATER
C
  PH2O=EXP(-2.424+0.0367*(TE-492.))
  PSOL2=14.696-PH2O
  DO 31 I=1,NCOMP
    SY(I)=1.0
  DO 600 J=1,NCOMP

```

```

IF(J=I) 610,600,610
610 SY(J)=0.0
600 CONTINUE
CALL PHIX(PSOL2,TR,ZV,SY)
SO(I)=EXP(2.3026*(-SA(I)+SB(I)/TK+SC(I))=ALOG(TK)/
1 2.3026))
AN(I)=SO(I)/(82.06*ZV*TK)
XM(I)=AN(I)/55.51
HENRS(I)=PSOL2*PHI(I)/XM(I)
PMOLV(I)=(C.0958+3.76*TR*PC(I)/(353156.*TC(I)))*(15.75
1 TC(I)/PC(I))
31 CONTINUE
DO 222 I=1,NCOMP
Y(I)=TEMPY(I)
DO 222 J=1,2
CLI(I,J)=ALI(I,J)/TK*EXP(BLI(I,J)/TK)
CLII(I,J)=ALII(I,J)/TK*EXP(BLII(I,J)/TK)
222 CONTINUE
C
C TEST IF IT IS A PURE COMPONENT
C
DO 700 I=1,NCOMP
MD=I
IF(Y(I)-1.0) 700,710,710
700 CONTINUE
GO TO 720
710 IF(CLII(MD,2)) 730,740,730
730 HI=-2.0
GO TO 48
740 HII=-2.0
GO TO 201
C
C TEST IF HYDRATE I WILL FORM
C
720 DO 200 I=1,NCOMP
IF(CLII(I,2)) 200,201,200
200 CONTINUE
HI=-2.0
GO TO 48,
C
C ASSUME HYDRATE I PRESENT IN WATER
C
48 PG=P
HI=HI+1.0
PII=P

```

```

DO 51 I=1,NCOMP
DO 51 J=1,2
CL(I,J)=CLI(I,J)
51 CONTINUE
PDELU=302.
DELHI=275.
DELHF=-1436.3
DELVI=3.0
DELVF=1.626
AR=-1212.2
BR=44344.0
CR=187.719
U(1)=UI(1)
U(2)=UI(2)
GO TO 30
C
C ASSUME HYDRATE II PRESENT IN WATER.
C
201 HII=HII+1.0
DO 4 I=1,NCOMP
DO 4 J=1,2
CL(I,J)=CLII(I,J)
4 CONTINUE
RDELU=211.
DELHI=193.
DELHF=-1436.3
DELVI=3.4
DELVF=1.626
U(1)=UII(1)
U(2)=UII(2)
IF(TK-291.) 5,5,5
5 AR=-1023.14
BR=34984.3
CR=159.923
GO TO 30
C AR=4071.64
BR=-193428.8
CR=-599.755
C
C CALCULATE THE CHEMICAL POTENTIAL DIFFERENCE OF THE
C REFERENCE HYDRATE
C
30 PGA=EXP(AR+BR/TK+CR*ALCG(TK))
PR=PGA
CALL QG10(TC,TK,AR,BR,CR,FI)
FI=DELHI*(1.0/TK-1.0/TG)

```

```

FII=FII+DAH*ALOG(TK/TC)+DEH*(TK-T0)-H*(1.0/TK-1.0/T0)
PO=EXP(AR+BR/T0+CR*ALOG(T0))
RDELU=RDELU+(DELVI+DELVF)*PG*0.024214
RDEL=TK*(RDELU/T0+FII+(DELVI+DELVF)*FI*0.024214)
P=PGA*14.696
PA=PGA

```

C
C CALCULATE GAS SOLUBILITY IN WATER
C

```

EPS=0.01
33 SUMXS=0.0
NOL=NOL+1
CALL PHIX(P,TR,ZV,Y)
DO 32 I=1,NCOMP
HEN(I)=EXP(ALOG(HENRS(I))+PMOLV(I)*(P-PH2O)/(10.73*
1,TR))
PHF(I)=PHI(I)*Y(I)*D
F(I)=PHF(I)/14.696
XS(I)=PHF(I)/HEN(I)
SUMXS=SUMXS+XS(I)
32 CONTINUE
XW=1.0-SUMXS
DO 40 J=1,2
TEMP(J)=0.0
DO 40 I=1,NCOMP
TEMP(J)=TEMP(J)+CL(I,J)*PHI(I)*Y(I)
40 CONTINUE

```

C
C USING NEWTON-RAPHSON METHOD TO SOLVE P
C

```

38 ASUM1=0.0
ASUM2=0.0
DO 39 J=1,2
SUM1(J)=U(J)*ALOG(1.0+TEMP(J)*PA)
ASUM1=ASUM1+SUM1(J)
SUM2(J)=U(J)*TEMP(J)/(1.0+TEMP(J)*PA)
ASUM2=ASUM2+SUM2(J)
39 CONTINUE
R1=1.9E7*TK*(ASUM1+ALOG(XW))-RDEL-(DELVI+DELVF)*(PA-PR
1)*0.024214
R2=1.987*TK*ASUM2-(DELVI+DELVF)*0.024214
R=R1/P2
PA=PA-R
RA=R/PA
ITER=ITER+1
IF(ITER>200) 680,690,690

```

```

690  RB=RA
      IF(LMT=200) 94,61,94
680  IF(ABS(RA)-EPS) 43,43,41
41   IF(PA) 42,42,38
42   PA=0.5*PGA
      GO TO 38
43   RB=(PA-PGA)/PA
      P=14.696*PA
      IF(ABS(RE)-0.001) 46,46,44
44   PGA=PA
      IF(ITER=200) 45,45,94
45   EPS=AES(0.1*RB)
      IF(EPS-0.01) 33,33,47
47   EPS=0.01
      GO TO 33
46   IF(HII) 58,49,43
49   IF(HI) 55,50,60
50   LMT=200
      GO TO 48
56   IF(P-PII) 57,56,61
61   P=PII
      WRITE(6,108) TF,P,ITER,NCL
      KIND=2
      GO TO 99
64   RB=RB*P
      WRITE(6,115)
      GO TO 45
65   WRITE(6,113) TF,P,ITER,NCL
      KIND=1
      GO TO 99
66   WRITE(6,111) TF,P,ITER,NCL
      GO TO 99
67   WRITE(6,113) TF,P,ITER,NCL
      KIND=1
      GO TO 99
68   WRITE(6,108) TF,P,ITER,NCL
      KIND=2
69   DO 170 I=1,NCOMP
170   WRITE(6,121) Y(I),(ALC(I,IN),IN=1,5)
      IF(KHC) 209,500,209
500   IF(NTC) 1000,10,1000
1000  TF=TF-DT
      IF(TF-32.) 10,999,999
C
C   CALCULATE HYDRATE COMPOSITION
C

```

```

209 IF(KIND-1) 205,205,207
205 DO 206 I=1,NCOMP
      DO 206 J=1,2
206 CL(I,J)=CLI(I,J)
      U(1)=UI(1)
      U(2)=UI(2)
      GO TO 240
207 DO 208 I=1,NCOMP
      DO 208 J=1,2
208 CL(I,J)=CLII(I,J)
      U(1)=UII(1)
      U(2)=UII(2)
      P=PII
240 DO 210 J=1,2
      SCF(J)=1.0
      DO 210 I=1,NCOMP
          F(I)=PHI(I)*Y(I)*P/14.696
          CF(I,J)=CL(I,J)*F(I)
          SCF(J)=SCF(J)+CF(I,J)
210 CONTINUE
      SSM=0.0
      DO 212 I=1,NCOMP
          SSML(I)=1.0E-8
          DO 211 J=1,2
              SML(I,J)=CF(I,J)/SCF(J)
              SSML(I)=SSML(I)+SML(I,J)*U(J)
211 CONTINUE
212 SSM=SSM+SSML(I)
      DO 220 I=1,NCOMP
220 HM(I)=SSML(I)/SSM
      WRITE(6,120)
      DO 230 I=1,NCOMP
230 WRITE(6,121) HM(I),(AL(I,IN),IN=1,S)
      GO TO 500
1001 CALL EXIT
100 FORMAT(3IS,F10.0)
101 FORMAT(5A4)
102 FORMAT(F10.0)
103 FORMAT(4E20.5)
104 FORMAT(2F10.5)
105 FORMAT(8F10.5)
108 FORMAT(/5X,'HYDRATE II WILL FORM AT' T=F6.1,
     1F',4X,'P=' ,F8.1,' PSIA',37X,'IT=' ,I5,3X,'OD=' ,I4)
113 FORMAT(/5X,'HYDRATE I WILL FORM AT' T=F6.1,
     1F',4X,'P=' ,F8.1,' PSIA',37X,'IT=' ,I5,3X,'OD=' ,I4)
111 FORMAT(/5X,'BOTH HYDRATE I AND II WILL FORM AT'

```

```

1 T=*,F6.1,  ' F',4X,'P=*,F8.1,* PSIA*,2GX,*IT=*,I5,3X,
2 *OD=*,I5)
112 FORMAT(7F10.0/3F10.0)
114 FORMAT(7F10.5/3F10.5//)
120 FORMAT(//10X,'THE HYDRATE COMPOSITION IS')
121 FORMAT(68X,F10.5,2X,5A4)
115 FORMAT(//10X,'THE PROGRAM COULD NOT CONVERGE AFTER 200
1 ITERATIONS'//15X,'DEVIATION IS ',F9.2,' PSIA')
END.

```

```

SUBROUTINE QG10(XL,XU,AR,BR,CR,FI)
FCT(T)=EXP(AR+BR/T+CR* ALOG(T))*(-BR/ T**3+CR/T**2)
A=.5*(XU+XL)
B=XU-XL
C=.4869533*B
Y=.03333567*(FCT(A+C)+FCT(A-C))
C=.4325317*B
Y=Y+.07472567*(FCT(A+C)+FCT(A-C))
C=.3397048*B
Y=Y+.1095432*(FCT(A+C)+FCT(A-C))
C=.2166977*B
Y=Y+.1346334*(FCT(A+C)+FCT(A-C))
C=.07443717*B
Y=B*(Y+.14777621*(FCT(A+C)+FCT(A-C)))
RETURN
END

```

```

SUBROUTINE PHIX(P,T,ZV,Y)
DIMENSION ARKV(4,4),BRKV(4),AIRKV(4),PHILN(4),A(4),
1 Z(3),Y(4),VCIJV(4,4),WIJ(4,4),ZCIJ(4,4)
COMMON PC(4),VC(4),TC(4),W(4),C1RKV(4),C2RKV(4),
1TCIJV(4,4),PCIJV(4,4),CORIJ(4,4),NCOMP,PHI(4)
C

```

C CALCULATE VAPOR-PHASE FUGACITY COEFFICIENTS USING
 C REVISED REDLICH AND KWONG EQUATION

C CALCULATE A AND B IN MODIFIED RK EQN FOR MIXTURE.

DO 100 I=1,NCOMP

ARKV(I,I)=C1RKV(I)*10.73**2*(TC(I)**2.5)/PC(I)

```

        BRKV(I)= C2RKV(I)*10.73*TC(I)/PC(I)
        IF (NCOMP -I) 111,110,111
111  II=I+1
        DO 100 J=II,NCOMP
          TCIJV(I,J)=(TC(I)*TC(J))**0.5*(1.0-CORIU(I,J))
          WIJ(I,J)=(W(I)+W(J))*0.5
          ZCIJ(I,J)=0.291-0.08*WIJ(I,J)
          VCIJV(I,J)=(VC(I)+VC(J))*0.5
          PCIJV(I,J)=ZCIJ(I,J)*10.73*TCIJV(I,J)/VCIJV(I,J)
          ARKV(I,J)=(C1RKV(I)+C1RKV(J))*0.5*10.73**2*TCIJV(I,J)
          1**2.5/PCIJV(I,J)
          ARKV(J,I)=ARKV(I,J)
100  CONTINUE
110  CONTINUE
        AMRKV=0.0
        BMRKV=0.0
        DO 120 I=1,NCOMP
          AIRKV(I)=0.0
          BMRKV=BMRKV+Y(I)*ERKV(I)
        DO 120 J=1,NCOMP
          AIRKV(I)=AIRKV(I)+Y(J)*ARKV(I,J)
120  AMRKV=AMRKV+Y(I)*Y(J)*ARKV(I,J)

C
C      CALCULATE VAPOR MOLAR VOLUME FOR MIXTURE.
C
        A(1)=1.0
        A(2)=-1.0
        RT= 10.73 *T
        PBRT=P*BMRKV/RT
        ABRT=AMRKV/(BMRKV*10.73*T**1.5)
        A(3)=PBRT*(ABRT-1.0=PERF)
        A(4)=ABRT*(PBRT**2)
C
        CALL CUBEG (A,MTYPE ,Z)
C
        IF (MTYPE) 130,140,14C
130  IF (Z(1) =Z(2)) 131,131,133
131  IF (Z(2)- Z(3)) 134,134,132
134  ZV=Z(3)
        GO TO 150
132  ZV=Z(2)
        GO TO 150
133  IF (Z(1)-Z(3)) 134,134,135
135  ZV=Z(1)
        GO TO 150
140  ZV=Z(1)

```

```

150 VV=ZV*RT/P
C
C      CALCULATE FUGACITY COEFFICIENTS WITH MODIFIED RK
C      EQUATION.
C
      QVVB=ALOG(VV/(VV-BMRKV))
      Q1VB=1.0/(VV-BMRKV)
      Q2RTB=2.0/(10.73*T**1.5*BMRKV)
      QVBV=ALOG((VV+BMRKV)/VV)
      QARTB=AMRKV/(10.73*T**1.5*BMRKV**2)
      QBVB=BMRKV/(VV+BMRKV)
      DO 160 I=1,NCOMP
      PHILN(I)=QVVB+BRKV(I)*Q1VB-AIRKV(I)*Q2RTB*CVRBV+BRKV(I)
      1*QARTB*(QVBV-QBVB)-ALOG(ZV)
      1-QBVB)-ALOG(ZV)
160 PHI(I)=EXP(PHILN(I))
      RETURN
      END

```

```

SUBROUTINE CUBEQ(A,MTYPE,Z)
C
C      SOLVES CUBIC REDLICH-KWONG EQUATION FOR COMPRESSIBILI-
C      TY FACTOR
C
      DIMENSION B(3),A(4),Z(3)
C
      B(1) = A(2)/A(1)
      B1OV3 = B(1)/3.0
      B(2) = A(3)/A(1)
      B(3) = A(4)/A(1)
      ALF = B(2) - B(1)*B1OV3
      BET = 2.0*B1OV3**3 - B(2)*B1OV3 + B(3)
      BETOV = BET/2.0
      ALFOV = ALF/3.0
      CUACV = ALFOV **3
      SQBOV = BETOV **2
      DEL = SQBOV + CUACV
      IF (DEL) 40,20,30
20 MTYPE = 0
      GAM = SQRT (-ALFOV )
      IF (BET) 22,22,21
21 Z(1) = -2.0*GAM -B1OV3
      Z(2) = GAM -B1OV3
      Z(3) = Z(2)

```

```

GO TO 50
22 Z(1) = 2.0*GAM - B10V3
Z(2) = -GAM - B10V3
Z(3) = Z(2)
GO TO 50
30 MTYPE = 1
EPS = SQRT (DEL)
TAU = -BETOV
RCU=TAU+EPS
SCU=TAU-EPS
SIR=1.0
SIS=1.0
IF (RCU) 31,32,32
31 SIR=-1.0
32 IF (SCU) 33,34,34
33 SIS=-1.0
34 R=SIR*(SIR*RCU)**0.33333333
S=SIS*(SIS*SCU)**0.33333333
Z(1) = R + S - B10V3
Z(2) = -(R+S)/2.0 - B10V3
Z(3) = 0.86602540*(R-S)
GO TO 50
40 MTYPE = -1
QUOT = SQBOV / CUAOV
ROOT = SQRT (-QUOT)
IF(BET) 42,41,*1
41 PEI = (1.5707963 + ATAN (ROOT / SQRT (1.0 - ROOT**2)))
1 / 3.0
GO TO 43
42 PEI = ATAN (SQRT (1.0 - ROOT**2) / ROOT) / 3.0
43 FACT = 2.0*SQRT (-ALFCOV )
Z(1) = FACT*COS (PEI) - B10V3
PEI=PEI+2.0943951
Z(2) = FACT*SIN(PEI) - B10V3
PEI=PEI+4.1887902
Z(3) = FACT*COS (PEI) - B10V3
50 CONTINUE
RETURN
END

```